Published in final edited form as:
J Immunol. 2012 September 15; 189(6): 2702–2706. doi:10.4049/jimmunol.1201682.

Intravascular staining redefines lung CD8 T cell responses[1]

Kristin G. Anderson[*], **Heungsup Sung**[*,†], **Cara N. Skon**[*], **Leo Lefrancois**[‡], **Angela Deisinger**[*], **Vaiva Vezys**[*], and **David Masopust**[*]

[*]Department of Microbiology, Center for Immunology, University of Minnesota, Minneapolis, MN 55455

[‡]Department of Immunology, University of Connecticut Health Center, Farmington, CT 06030

Abstract

Non-lymphoid T cell populations control local infections and also contribute to inflammatory diseases, thus driving efforts to understand the regulation of their migration, differentiation, and maintenance. Numerous observations indicate that T cell trafficking and differentiation within the lung is starkly different than what has been described in most non-lymphoid tissues, including intestine and skin. We found that >95% of memory CD8 T cells isolated from mouse lung via standard methods were actually confined to the pulmonary vasculature, despite perfusion. Respiratory route of challenge increased virus specific T cell localization within lung tissue, although only transiently. Removing blood-born cells from analysis by the simple technique of intravascular staining revealed distinct phenotypic signatures and chemokine-dependent trafficking that was restricted to antigen-experienced T cells. These results precipitate a revised model for pulmonary T cell trafficking and differentiation and a re-evaluation of studies examining the contributions of pulmonary T cells to protection and disease.

Introduction

A dense network of pulmonary capillaries underlying the alveoli forms the structural basis of respiration. Gas exchange is most efficient at the thinnest portions of the air-blood barrier where narrow capillaries share a fused basal lamina with alveolar epithelium. This intimate association between the capillary bed, a thin permeable membrane, and the outside world, coupled with the fact that inflammation can disrupt the delicate architecture necessary for gas exchange, creates vulnerabilities. Indeed, lower respiratory infections account for the single greatest cause of death from infectious disease, and the incidence of chronic T cell dependent inflammatory diseases such as asthma are increasing (1, 2).

T cell differentiation is coupled with anatomic distribution. Naïve and central memory T cells (T_{CM}) recirculate through secondary lymphoid organs, blood, and lymphatic vessels. This restricted homing pattern optimizes interaction with professional APCs and subsequent proliferation in response to cognate antigen recognition. Effector memory T cells (T_{EM}) patrol non-lymphoid tissues where they are positioned for more immediate interception of pathogens at the most common points of exposure (3). Indeed, resident T_{EM} within skin contribute most rapidly to control of local re-infection (4, 5). Resident T_{EM} populations have

[1]This study was funded by R01AI084913 (DM), the Beckman Young Investigator Award (DM), and NIH Immunology grant T32-AI07313 (CNS). The authors have no conflicting financial interests.

Correspondence: Dr. David Masopust, University of Minnesota, 2101 6th Street SE, Minneapolis, MN 55455, Phone: 612-625-4666, Fax: 612-625-2199, masopust@umn.edu.
[†]Present Address: Department of Laboratory Medicine, Asan Medical Center and University of Ulsan College of Medicine, 88, Olympic-ro 43-gil, Songpa-gu, Seoul, 138-736, South Korea

been defined in many non-lymphoid tissues, and are characterized by unique phenotypic signatures not represented in blood, including CD69 and CD103/β7 integrin (4–8).

Regardless of route, infection or immunization gives rise to extraordinarily large effector and memory T cell populations that can be isolated from perfused mouse lung (9, 10). However, lung T cell migration and differentiation is less clear than in tissues such as the intestinal mucosa, skin, brain, or lymph nodes (LNs). In contrast to the stereotypic 3-step model of lymphocyte extravasation (11), some evidence demonstrates that T cell homing to lung is chemokine-independent (12). However, expression of chemokine receptors by T cells, including CCR5 and CXCR3, are required for normal distribution and differentiation of lung T cells following local infection (13). In some infection models, the lung contains a large fraction of T_{CM} (14). In fact, even naïve lymphocytes can be isolated from the perfused lung (15–17). These observations contrast with most other non-lymphoid compartments, which do not contain T_{CM}, exclude naïve T cells, and require chemokine signaling for entry. This study sheds light on these issues by refining our understanding of the anatomic compartmentalization of CD8 T cells within the lung.

Materials and Methods

Mice and infections

P14 chimeric immune mice were generated as described (6). Mice were either infected intraperitoneally (i.p.) with 2×10^5 PFU LCMV or intratracheally (i.t.) with 1×10^5 PFU LCMV (18). The University of Minnesota IACUC approved all experiments.

Intravascular staining and cell isolations

3 μg of Anti-CD8a-APC or anti-CD8a-PE (clone: 53-6.7 from eBioscience) or purified rabbit anti-mouse collagen IV (Novus Biologicals) were injected intravenously (i.v.). Three minutes later, the animals were sacrificed, lavaged to remove cells in the airway, bled, and perfused with 10 ml of cold PBS. The spleen, LNs, lung, liver, and small intestine were harvested within 12min, and lymphocytes were isolated as described (19). Immunofluorescence staining was performed as described (6).

Pertussis Toxin Treatment

Purified splenocytes from P14 immune chimeric mice or naïve P14 transgenic mice were incubated in RPMI containing 10% FBS +/− 25 ng/ml pertussis toxin (R&D Systems) at a concentration of 1.5×10^7 cells/ml for 1h at 37°C as described (8). Following incubation, $1.5–3.5\times10^7$ cells were injected i.v. into C57Bl/6 recipient mice.

Results and Discussion

Pertussis toxin treatment of T cells yields increased recovery from lung

We wished to confirm the pertussis toxin (PTx) sensitivity of memory CD8 T cell homing to lung and other tissues, and also to address this issue for naïve CD8 T cells. Gp33-specific P14 memory CD8 T cells were generated in vivo in response to i.p. lymphocytic choriomeningitis virus (LCMV) infection (referred to hereafter as P14 immune chimeras, see methods). Eight weeks later, splenocytes containing memory P14 CD8 T cells were treated with PTx or control media, then transferred i.v. into naïve recipients. Three days after transfer, various tissues were harvested to assess T cell migration. Consistent with the known requirement for CCR7, migration to inguinal LN (ILN) was blocked by PTx treatment, and there was a reciprocal increase of donor cells among spleen and PBL. As reported previously, PTx treatment did not inhibit migration to lung, and like blood, actually led to an increase in recovered cells (Fig. 1A). This experiment was repeated with naïve P14

CD8 T cells with similar results (Fig. 1B). These data suggest that even naïve CD8 T cells home to lung in a chemokine independent process, particularly when LN homing was inhibited.

In vivo staining distinguishes between anatomic compartments

We wished to define which lung compartment naïve T cells migrated to. We injected anti-CD8α antibody (Ab) i.v into naïve mice that had received untreated naïve P14 CD8 T cells. Three minutes later, blood was isolated, mice were immediately sacrificed and perfused with PBS, and tissues were quickly dissected, minced, and rinsed of free Ab. Lymphocytes were isolated via standard methods then stained with anti-CD8α surface Ab and other markers of interest. The permissiveness of donor naïve T cells to i.v. staining varied among distinct tissues (Fig. 2A): 100% of donor cells within blood, a subset of cells within spleen, and virtually no cells within LN were labeled. Like blood, 100% of naïve donor cells isolated from lung labeled with injected anti-CD8α Ab. PTx treatment increased the number of labeled donor cells recovered from blood, spleen and lung, but reduced the number of unlabeled cells recovered from spleen and ILN (Fig. 2B).

To assess whether intravascular staining was associated with distinct anatomic compartments, we injected anti-CD8α-PE Ab into P14 immune chimeras, sacrificed and perfused recipients, then immediately froze spleen and lung for immunofluorescence. Injected Ab labeled CD8 T cells in red pulp but not those in white pulp of spleen (Fig. 2C). Lung tissue sections were also surface stained for CD8α-AF488, CD31-AF647 (which labels vascular endothelium), and DAPI (which labels cell nuclei). Analysis of the lung revealed that the vast majority of CD8 T cells were labeled only with injected Ab (Fig. 2D). Closer inspection revealed that these cells (red) appeared to be closely associated with pulmonary capillaries (blue, Fig. 2E&F). These data indicate that most cells were exposed to injected Ab, and that in vivo staining blocked ex vivo surface staining on tissue sections. However, a small fraction of CD8α+ cells, typically surrounding airways and large blood vessels, were only labeled by ex vivo staining (green) of tissue sections, suggesting that they were protected from i.v. injected Ab (Fig. 2G&H).

Migration to uninflamed lung tissue is chemokine dependent

Based on these data, it was possible that intravascular labeling of cells in the lung was restricted to cells contained within pulmonary capillaries or other blood vessels that were refractory to removal by perfusion. Alternatively, injected Ab may have leaked or been exported out of the pulmonary capillary bed, thereby staining perivascular cells. A collagen IV containing basement membrane underlies the lung vascular endothelium (as revealed by surface staining, Fig. 3A, upper right panel). We injected anti-collagen IV Ab and found that the basement membrane remained unlabeled, suggesting that the capillary bed did not allow rapid perivascular leakage of Abs (Fig. 3A, lower right panel). For controls, we examined surface and injected collagen IV staining in the spleen (where only red pulp was exposed to injected Ab) and liver (which contains fenestrated endothelium within sinusoids, which permitted intravascular staining of basement membrane, Fig. 3A).

To further test the interpretation that intravascular staining identifies cells contained within the capillary bed of the lungs of perfused mice, we revisited the issue of PTx insensitive lung trafficking. As in Fig. 1A, PTx-treated or control memory CD8 T cells were transferred i.v. and recipient tissues were harvested three days later. The vast majority of untreated donor cells harvested from lung became labeled with injected Ab. However, a small fraction (~6%) was within a compartment of the lung that was protected from injected Ab. Importantly, appearance of this subset was PTx sensitive (Fig. 3B&C), suggesting that it represented a chemokine dependent trafficking event.

Most lung memory CD8 T cells are capillary-associated after infection

Our results thus far indicate that the vast majority of transferred CD8 T cells recovered from perfused lung were actually present within the narrow capillary network associated with alveoli. We next sought to determine what proportion of memory CD8 T cells recovered from the lungs of infected mice were within blood. To this end, we generated P14 immune chimeras using an i.p. route of infection. We found that >96% of LCMV-specific CD8 T cells isolated from the lung were labeled with intravascular Ab (Fig. 4A). To determine whether this vascular-biased localization was unique to an i.p. infection, mice were instead infected via the intratracheal (i.t.) route. Although local infection established a significantly greater CD8 T cell response in the lung stroma and inducible bronchus-associated lymphoid tissue (iBALT), the majority of cells isolated from lung were still capillary-derived (Fig. 4A).

After infection, mice inoculated i.p. maintained a constant proportion of P14 CD8 T cells in the lung tissue vs. capillaries. In contrast, i.t. infected mice experienced a dynamic elevation and contraction in the proportion of P14 CD8 T cells within lung tissue relative to capillaries (Fig. 4B), correlating with the transient presence of iBALT (data not shown). In spleen, P14 CD8 T cells initially predominated in red pulp, then gradually shifted to white pulp (Fig. 4B), correlating with T_{CM} differentiation (20).

Differential phenotype of lung tissue and vascular CD8 T cells

We then examined the phenotype of P14 CD8 T cells 15 days after i.t. LCMV infection. P14 cells present in peripheral blood bore a striking resemblance to those cells isolated from the lung that stained with injected Ab (Fig. 4C–F, rows 1 and 2). In contrast, cells protected from i.v. staining were distinct, contained subsets of CD103+ and CD69+ cells, and were uniformly CXCR3+ (Fig 4C–F, rows 2 and 3). Airway T cells (removed prior to lung digestion) exhibited a distinct phenotype, including pronounced down-regulation of CD11a as previously described (Fig. 4C–F, rows 3 and 4) (21). P14 CD8 T cells isolated from the liver or small intestine epithelium that were protected from i.v. staining (~5% or >99% of total P14s isolated from each tissue, respectively, data not shown) were also uniformly CXCR3+ but were distinct from lung tissue cells in many respects (Fig. 4C–F, rows 5 and 6).

A previous report quite elegantly demonstrated that CD8 T cells stimulated in vitro under varying conditions, and then transferred i.v., were differentially labeled by intravascular staining when recovered from lung, and exhibited distinct homing requirements (22). Our study validates that intravascular staining discriminates between CD8 T cells present within the lung tissue from those trapped in the vasculature. We utilized this approach to re-evaluate the anatomic distribution of CD8 T cells isolated from lung after in vivo infection. This analysis revealed the major finding that, in some contexts, up to 96% of effector or memory T cells isolated from lung represent cells in the capillary vessels rather than lung tissue. Unique phenotypic signatures were expressed among cells protected from labeling, including CD69 and CD103/β7 integrin expression, which has been associated with resident T_{EM} populations (4–7). Moreover, only a small fraction of memory CD8 T cells transferred into naïve recipients that were recovered from lung actually migrated into the tissue. This process was chemokine dependent, and naïve T cells were excluded. These results precipitate a re-evaluation of previous studies that examined the distribution, phenotype, and homing requirements of pulmonary T cells, and also have ramifications for T cell-dependent protection studies that may overestimate localization of transferred or established T cell populations within lung tissue (20, 23). The development of vaccine modalities that enhance true T cell homing to lung tissue, which may be evaluated by intravascular staining, may enhance protection against respiratory infections (24–26).

In summary, our results demonstrate that intravascular staining is a useful tool to define vascular and tissue pulmonary lymphocytes, indicate that the majority of T cells are often within the vasculature of perfused lung, and support a revised model of the regulation of cellular immunity within the respiratory mucosa.

Acknowledgments

We thank Jeff Hogan for advice on i.t. immunization, and M Jenkins, S Jameson, and K Hogquist for helpful discussion.

References

1. WHO. Geneva: 2004. The World Health Report: 2004, Changing History.
2. Holgate ST. Innate and adaptive immune responses in asthma. Nat. Med. 2012; 18:673–683. [PubMed: 22561831]
3. Masopust D, Picker LJ. Hidden memories: frontline memory T cells and early pathogen interception. J. Immunol. 2012; 188:5811–5817. [PubMed: 22675215]
4. Gebhardt T, Wakim LM, Eidsmo L, Reading PC, Heath WR, Carbone FR. Memory T cells in nonlymphoid tissue that provide enhanced local immunity during infection with herpes simplex virus. Nat. Immunol. 2009; 10:524–530. [PubMed: 19305395]
5. Jiang X, Clark RA, Liu L, Wagers AJ, Fuhlbrigge RC, Kupper TS. Skin infection generates non-migratory memory CD8+ T(RM) cells providing global skin immunity. Nature. 2012; 483:227–231. [PubMed: 22388819]
6. Casey KA, Fraser KA, Schenkel JM, Moran A, Abt MC, Beura LK, Lucas PJ, Artis D, Wherry EJ, Hogquist K, Vezys V, Masopust D. Antigen-Independent Differentiation and Maintenance of Effector-like Resident Memory T Cells in Tissues. J. Immunol. 2012; 188:4866–4875. [PubMed: 22504644]
7. Wakim LM, Woodward-Davis A, Bevan MJ. Memory T cells persisting within the brain after local infection show functional adaptations to their tissue of residence. Proc. Natl. Acad. Sci. USA. 2010; 107:17872–17879. [PubMed: 20923878]
8. Masopust D, Choo D, Vezys V, Wherry EJ, Duraiswamy J, Akondy R, Wang J, Casey KA, Barber DL, Kawamura KS, Fraser KA, Webby RJ, Brinkmann V, Butcher EC, Newell KA, Ahmed R. Dynamic T cell migration program provides resident memory within intestinal epithelium. J. Exp. Med. 2010; 207:553–564. [PubMed: 20156972]
9. Marshall DR, Turner SJ, Belz GT, Wingo S, Andreansky S, Sangster MY, Riberdy JM, Liu T, Tan M, Doherty PC. Measuring the diaspora for virus-specific CD8+ T cells. Proc. Natl. Acad. Sci. USA. 2001; 98:6313–6318. [PubMed: 11344265]
10. Masopust D, Vezys V, Marzo AL, Lefrancois L. Preferential localization of effector memory cells in nonlymphoid tissue. Science. 2001; 291:2413–2417. [PubMed: 11264538]
11. Bromley SK, Mempel TR, Luster AD. Orchestrating the orchestrators: chemokines in control of T cell traffic. Nat. Immunol. 2008; 9:970–980. [PubMed: 18711434]
12. Klonowski KD, Williams KJ, Marzo AL, Blair DA, Lingenheld EG, Lefrancois L. Dynamics of blood-borne CD8 memory T cell migration in vivo. Immunity. 2004; 20:551–562. [PubMed: 15142524]
13. Kohlmeier JE, Miller SC, Smith J, Lu B, Gerard C, Cookenham T, Roberts AD, Woodland DL. The chemokine receptor CCR5 plays a key role in the early memory CD8+ T cell response to respiratory virus infections. Immunity. 2008; 29:101–113. [PubMed: 18617426]
14. Unsoeld H, Pircher H. Complex memory T-cell phenotypes revealed by coexpression of CD62L and CCR7. J. Virol. 2005; 79:4510–4513. [PubMed: 15767451]
15. Cose S, Brammer C, Khanna KM, Masopust D, Lefrancois L. Evidence that a significant number of naive T cells enter non-lymphoid organs as part of a normal migratory pathway. Eur. J. Immunol. 2006; 36:1423–1433. [PubMed: 16708400]

16. Hofmann M, Brinkmann V, Zerwes HG. FTY720 preferentially depletes naive T cells from peripheral and lymphoid organs. Int. Immunopharmacol. 2006; 6:1902–1910. [PubMed: 17161343]

17. Harp JR, Onami TM. Naive T cells re-distribute to the lungs of selectin ligand deficient mice. PLoS One. 2010; 5:e10973. [PubMed: 20532047]

18. Hogan RJ, Zhong W, Usherwood EJ, Cookenham T, Roberts AD, Woodland DL. Protection from respiratory virus infections can be mediated by antigen-specific CD4(+) T cells that persist in the lungs. J. Exp. Med. 2001; 193:981–986. [PubMed: 11304559]

19. Masopust D, Vezys V, Wherry EJ, Barber DL, Ahmed R. Cutting edge: gut microenvironment promotes differentiation of a unique memory CD8 T cell population. J. Immunol. 2006; 176:2079–2083. [PubMed: 16455963]

20. Wherry EJ, Teichgraber V, Becker TC, Masopust D, Kaech SM, Antia R, von Andrian UH, Ahmed R. Lineage relationship and protective immunity of memory CD8 T cell subsets. Nat. Immunol. 2003; 4:225–234. [PubMed: 12563257]

21. Ely KH, Roberts AD, Woodland DL. Cutting edge: effector memory CD8+ T cells in the lung airways retain the potential to mediate recall responses. J. Immunol. 2003; 171:3338–3342. [PubMed: 14500625]

22. Galkina E, Thatte J, Dabak V, Williams MB, Ley K, Braciale TJ. Preferential migration of effector CD8+ T cells into the interstitium of the normal lung. J. Clin. Invest. 2005; 115:3473–3483. [PubMed: 16308575]

23. Gallegos AM, Pamer EG, Glickman MS. Delayed protection by ESAT-6-specific effector CD4+ T cells after airborne M. tuberculosis infection. J. Exp. Med. 2008; 205:2359–2368. [PubMed: 18779346]

24. Moyron-Quiroz JE, Rangel-Moreno J, Kusser K, Hartson L, Sprague F, Goodrich S, Woodland DL, Lund FE, Randall TD. Role of inducible bronchus associated lymphoid tissue (iBALT) in respiratory immunity. Nat. Med. 2004; 10:927–934. [PubMed: 15311275]

25. Teijaro JR, Turner D, Pham Q, Wherry EJ, Lefrancois L, Farber DL. Cutting edge: Tissue-retentive lung memory CD4 T cells mediate optimal protection to respiratory virus infection. J. Immunol. 2011; 187:5510–5514. [PubMed: 22058417]

26. Strutt TM, McKinstry KK, Dibble JP, Winchell C, Kuang Y, Curtis JD, Huston G, Dutton RW, Swain SL. Memory CD4+ T cells induce innate responses independently of pathogen. Nat. Med. 2010; 16:558–564. [PubMed: 20436484]

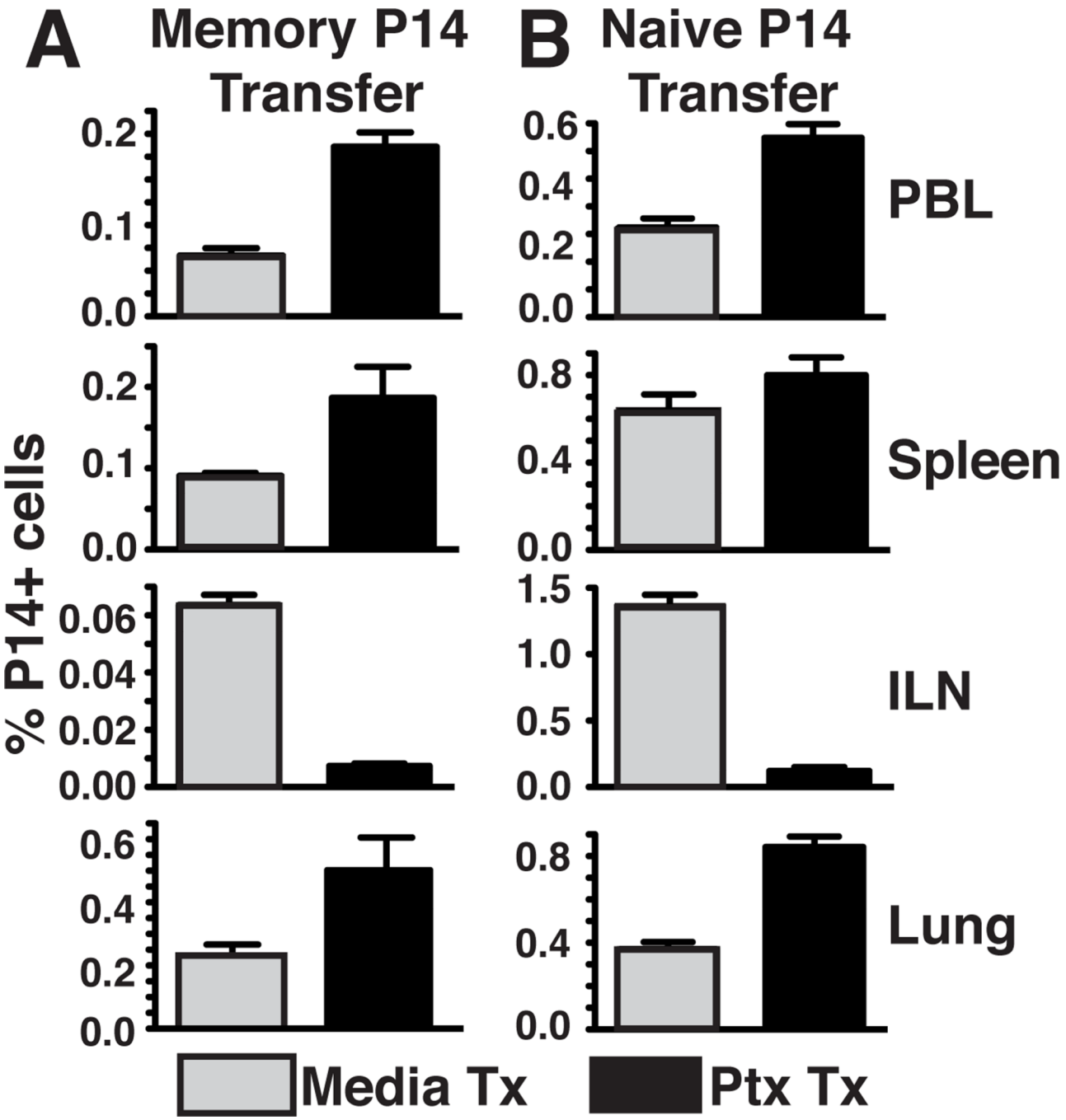

Figure 1. Pertussis toxin treatment of transferred T cells yields increased recovery from lung

Naïve or memory P14 splenocytes were treated with pertussis toxin (PTx) or media control and transferred i.v. into naïve recipients. Tissues were harvested 1 (naïve) or 3 (memory) days post-transfer. Frequency of memory (A) or naïve (B) P14 cells in PBL, spleen, ILN, or lung. Data are representative of 3 independent experiments totaling >12 mice/condition. Error bars indicate SEM.

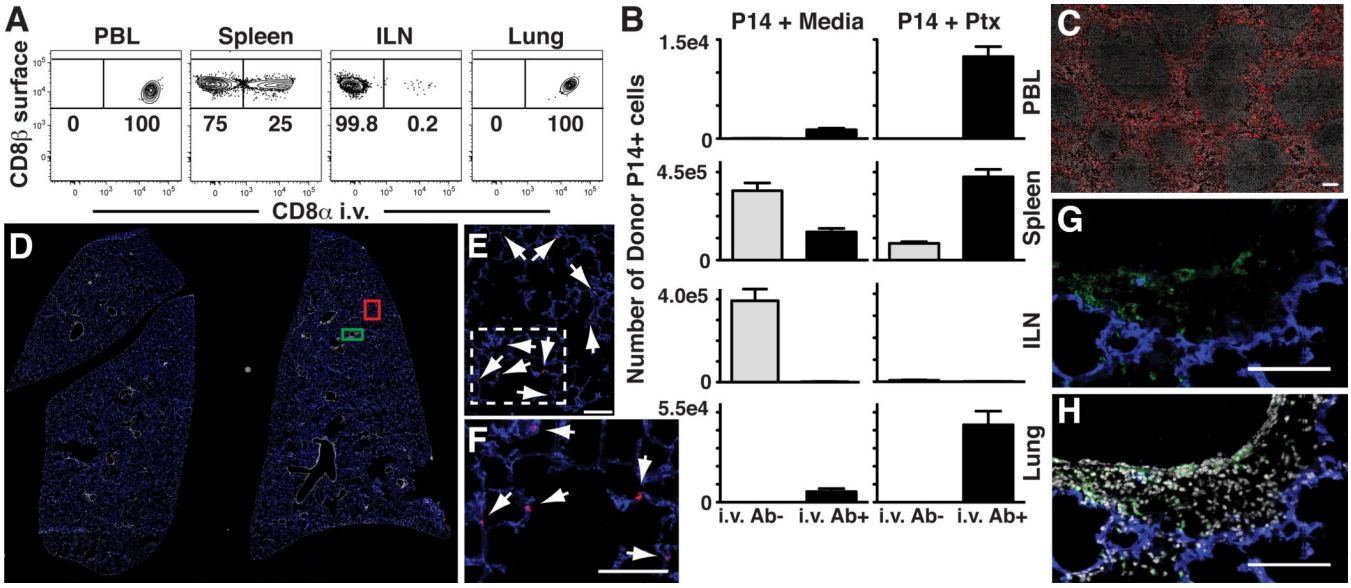

Figure 2. In vivo staining distinguishes between anatomic compartments

(A) Naïve Thy1.1+ P14 splenocytes were transferred i.v. into C57Bl/6J mice. Anti-CD8α was injected i.v. Three minutes later, tissues were harvested. Cells were isolated and then stained ex vivo with anti-CD8β. Plots gated on Thy1.1+ lymphocytes. (B) Number of i.v. Ab+ and i.v. Ab− naïve P14 cells, ± PTx treatment, isolated from tissues after transfer. (C) Spleen after anti-CD8α-PE i.v. injection. (D–H) Whole lung sections of P14 immune chimeras were imaged. Panels E and F or G and H represent enlarged images defined by red or green boxes, respectively, in panel D. CD8 T cells that stain with i.v. injected Ab (red) co-localize with blood vessels (CD31, blue, see E and enlarged inset F), whereas those protected from i.v. Ab (green surface stain) are spatially distinct (G and H, ± DAPI, respectively). Arrows designate red i.v. Ab+ cells. (A and B) are representative of 3 independent experiments totaling ≥12 mice/condition. Error bars indicate SEM. Images are representative of 2 independent experiments totaling 6 mice. Scale bars in C, E–H represent 100μm.

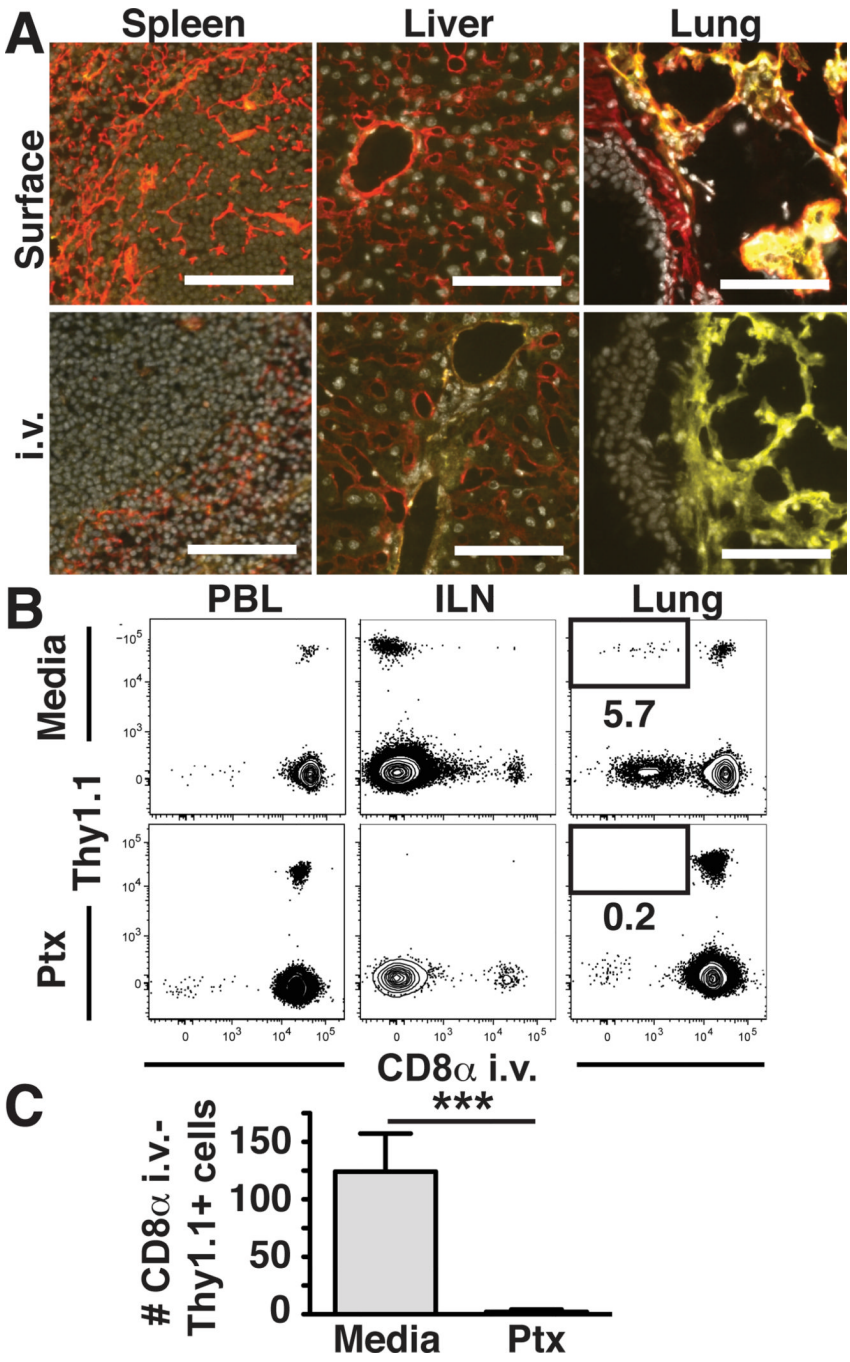

Figure 3. Migration of memory CD8 T cells to uninflamed lung tissue is chemokine dependent

(A) Anti-collagen IV Ab (red) was injected i.v. prior to tissue harvest or tissue sections were surface stained ex vivo along with anti-CD31 (yellow) and DAPI (gray). (B&C) Thy1.1+ memory P14 splenocytes were treated with PTx or media and transferred i.v. into naïve C57Bl/6J mice. Intravascular anti-CD8α staining and tissue harvest occurred 3 days later. (B) Representative flow cytometric analysis of the indicated recipient tissues. Plots gated on CD8β+ lymphocytes. (C) Number of donor memory P14 cells recovered from lung that were protected from intravascular staining (intravascular anti-CD8α negative). Images are representative of 2 independent experiments totaling 4 mice. Scale bars represent 100μm.

Plots in (B) and (C) are representative of 3 independent experiments totaling ≥12 mice/condition. ***, P=0.006 unpaired Student's t test. Error bars represent SEM.

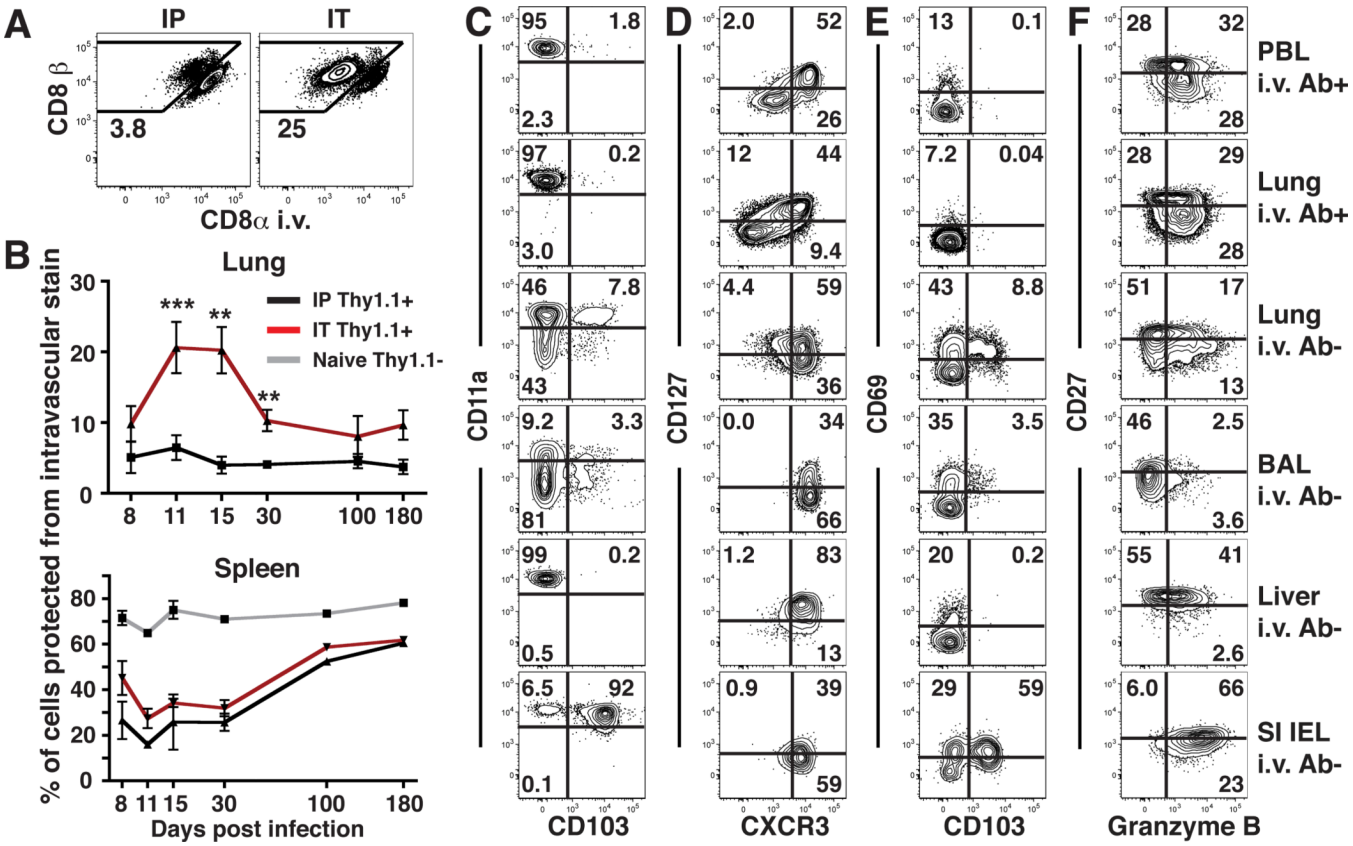

Figure 4. Most lung memory CD8 T cells are capillary-associated after infection

(A) P14 immune chimeras were infected with LCMV via the i.p. or i.t. route. 15 days later, mice were subject to intravascular staining (as in Fig. 2), and lymphocytes were isolated from perfused lung. Plots are gated on Thy1.1+ P14 cells. (B) Frequency of P14 cells that were protected from intravascular staining isolated from lung or spleen after i.p (black) or i.t. (red) infection. Proportion of naïve (CD44lo) CD8 T cells (gray) that were protected from intravascular staining was also determined in spleen. (C–F) The phenotype of P14 cells was evaluated in the indicated tissues 15 days after i.t. LCMV infection. Data are representative of 2–3 independent experiments per time point totaling ≥8 mice per condition. ***, P=0.0003; **, P<0.006 unpaired Student's t test. Error bars represent SEM.